JACS
JOURNAL OF THE AMERICAN CHEMICAL SOCIETY

ARTICLE

pubs.acs.org/JACS

(*E*)-Alkene and Ethylene Isosteres Substantially Alter the Hydrogen-Bonding Network in Class II MHC A^q/Glycopeptide Complexes and Affect T-Cell Recognition

Ida E. Andersson,[†] Tsvetelina Batsalova,[‡] Sabrina Haag,[‡] Balik Dzhambazov,[‡] Rikard Holmdahl,[‡] Jan Kihlberg,[*,†,§] and Anna Linusson[*,†]

[†]Department of Chemistry, Umeå University, SE-901 87 Umeå, Sweden

[‡]Medical Inflammation Research, Department of Medical Biochemistry and Biophysics, Karolinska Institute, SE-171 77 Stockholm, Sweden

[§]AstraZeneca Research and Development Mölndal, SE-431 83 Mölndal, Sweden

Supporting Information

ABSTRACT: The structural basis for antigen presentation by class II major histocompatibility complex (MHC) proteins to $CD4^+$ T-cells is important for understanding and possibly treating autoimmune diseases. In the work described in this paper, (*E*)-alkene and ethylene amide-bond isosteres were used to investigate the effect of removing hydrogen-bonding possibilities from the CII259−270 glycopeptide, which is bound by the arthritis-associated murine A^q class II MHC protein. The isostere-modified glycopeptides showed varying and unexpectedly large losses of A^q binding that could be linked to the dynamics of the system. Molecular dynamics (MD) simulations revealed that the backbone of CII259−270 and the A^q protein are able to form up to 11 hydrogen bonds, but fewer than this number are present at any one time. Most of the strong hydrogen-bond interactions were formed by the N-terminal part of the glycopeptide, i.e., in the region where the isosteric replacements were made. The structural dynamics also revealed that hydrogen bonds were strongly coupled to each other; the loss of one hydrogen-bond interaction had a profound effect on the entire hydrogen-bonding network. The A^q binding data revealed that an ethylene isostere glycopeptide unexpectedly bound more strongly to A^q than the corresponding (*E*)-alkene, which is in contrast to the trend observed for the other isosteres. Analysis of the MD trajectories revealed that the complex conformation of this ethylene isostere was structurally different and had an altered molecular interaction pattern compared to the other A^q/glycopeptide complexes. The introduced amide-bond isosteres also affected the interactions of the glycopeptide/A^q complexes with T-cell receptors. The dynamic variation of the patterns and strengths of the hydrogen-bond interactions in the class II MHC system is of critical importance for the class II MHC/peptide/TCR signaling system.

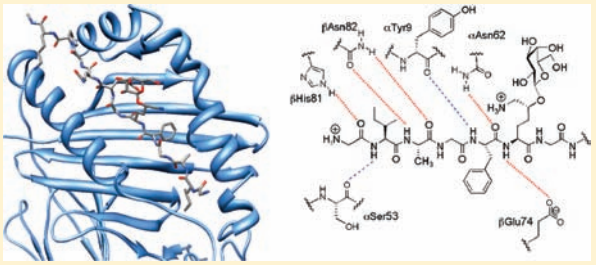

INTRODUCTION

Class II major histocompatibility complex (MHC) glycoproteins are expressed in antigen-presenting cells (APCs) where they bind peptide antigens derived from processing proteins of extracellular origin.[1] The resulting class II MHC/peptide complexes are transported to the cell surface of the APCs where they are presented to T-cell receptors (TCRs) on $CD4^+$ T-helper cells. The interactions governing the ternary class II MHC/peptide/TCR complexes play a crucial role in determining if an immune response is initiated via activation of the T-cell. Knowledge of the structural basis for antigen presentation by the class II MHC protein[2] and recognition by the TCR are important for understanding and possibly treating autoimmune diseases, such as type 1 diabetes, multiple sclerosis (MS), and rheumatoid arthritis (RA), where the immune system recognizes and attacks endogenous tissues.

Peptides consisting of up to 20 amino acid residues bind in an extended conformation in the class II MHC binding groove, which is open at both ends, allowing long peptides to protrude out of the groove.[2,3] A class II MHC protein can bind a variety of different peptides and present them to TCRs. This binding promiscuity is enabled by an array of sequence-independent hydrogen bonds formed between the peptide backbone and the MHC protein, while the specificity displayed by different class II MHC proteins is achieved through pockets in the MHC binding groove that have preferences for certain peptide amino acid side chains.[2]

The structure and the dynamics of class II MHC/peptide complexes have been studied through molecular dynamics (MD) simulations of the motions of the interacting atoms.[4−12] This information has been used to interpret biological processes regulated by class II MHC/peptide complexes on a molecular level. For example, structures extracted from MD simulations

Received: April 27, 2011
Published: July 18, 2011

were used in combination with binding affinity predictions and analysis of the hydrogen-bonding network to explain the variation in class II MHC binding between related peptides.[6] Although most MD simulations only include class II MHC/peptide complexes and not TCRs because of the limited number of TCR crystal structures, such data can still provide information about the T-cell responses.[5,7−9] For example, the exposed peptide surface area derived from MD data for a series of class II MHC-bound substituted hen egg lysozyme (HEL) peptides was correlated with their T-cell responses.[5] Furthermore, conformational changes in the MHC binding of different peptides observed in MD simulations have been linked to T-cell responsiveness and experimental autoimmune encephalomyelitis (EAE) induction in vivo.[7] We have recently linked flexibility and changes in the presented epitope of MHC anchor-modified glycopeptides to different T-cell responses.[11] Recently, parts of the TCR were included in a simulation of a homology model of an RA-associated TCR Vβ domain docked to a peptide/DR4 crystal structure, which indicated that certain residues of the flexible complementarity determining region (CDR)3β loop were critical for TCR recognition.[12]

To probe interactions in the ternary class II MHC/peptide/TCR complexes and also overcome some of the limitations associated with the therapeutic use of peptides, e.g., low bioavailability and metabolic stability, different modifications have been incorporated into peptides that interact with class II MHC proteins.[13−27] Examples include replacement of backbone amides by different amide bond isosteres (e.g., retro-inverso[16] and (*E*)-alkene)[15] or introduction of D-amino acids,[14] aza-amino acids,[21] and other non-natural amino acids.[20,24] There are also examples where modified peptides have been shown to prevent or treat disease in animal models for RA and MS.[13,23]

Vaccination of mice with glycopeptide **1** (Figure 1) alone[28] or in complex with the class II MHC A^q protein[29] has been shown to prevent development of collagen-induced arthritis (CIA), a mouse model for RA. This glycopeptide, which is a fragment from type II collagen (CII), was also recognized by T-cells isolated from a cohort of RA patients.[30] Comparative models[25,26] of the A^q/glycopeptide complex have revealed an extensive hydrogen-bonding network between the glycopeptide backbone and the residues in A^q. Furthermore, the Ile^{260} and Phe^{263} residues in **1** are anchored in the P1 and P4 pockets of A^q, whereas the β-D-galactopyranosyl hydroxylysine ($GalHyl^{264}$) side chain protrudes out of the binding site and is critical for recognition by the TCR (Figure 1).[31−33]

In this study we investigated the effect of removing backbone hydrogen-bonding possibilities from **1** on A^q binding and recognition by T-cell hybridomas. Glycopeptide **1** was modified by introducing (*E*)-alkene and ethylene isosteres instead of each of the three amide bonds in between the two anchors, Ile^{260} and Phe^{263} (Figure 1). These isostere moieties can mimic the geometry of the amide bond but lack hydrogen-bonding capability.[34] The inclusion of the ethylene isostere also enabled the effect of increasing the flexibility of the peptide backbone to be studied. The structural dynamics of the glycopeptide/A^q complexes were studied by MD simulations and compared to experimental results for A^q binding and T-cell responses.

RESULTS AND DISCUSSION

Synthesis. This study required synthesis of the dipeptide building blocks **2**−**7** (Figure 2), which were used to assemble

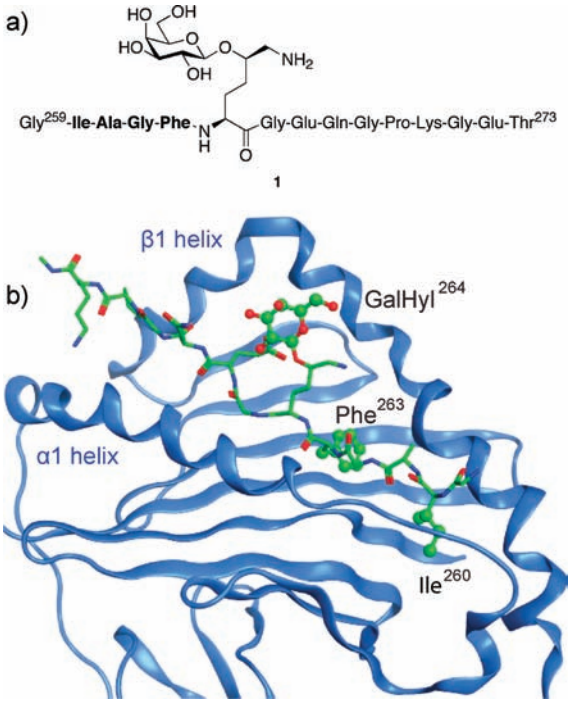

Figure 1. (a) Structure of glycopeptide **1** (CII259−273). The peptide sequence that was modified by (*E*)-alkene and ethylene isosteres in the present study is shown in bold. (b) Comparative model[25,26] of the complex between CII259−270 and the A^q protein. The A^q binding site has a secondary structure consisting of two parallel α helices (α1 and β1) on top of a β sheet. The glycopeptide **1** is bound in an extended backbone conformation with the $GalHyl^{264}$ side chain solvent exposed and the side chains of Ile^{260} and Phe^{263} buried in the P1 and P4 pocket, respectively. The side chains of $GalHyl^{264}$, Ile^{260}, and Phe^{263} are indicated by balls and sticks.

isosteric analogues of glycopeptide **1** using Fmoc-based solid-phase synthesis. The synthesis of Ile-Ala (*E*)-alkene and ethylene derivatives **2** and **3** was based on a strategy developed by Luthman and co-workers (Scheme 1).[35] Phosphonium salt **11** was first prepared via a three-step process: *N*-trifluoroacetyl protection of (*S*)-isoleucinol (**8**), conversion of the alcohol into the corresponding bromide (**10**), and displacement with triphenylphosphine. In the following Wittig reaction,[35] **11** was treated with *n*-butyllithium and reacted with chiral aldehyde **12**,[36,37] which afforded (*E*)-alkene **13** as a single stereoisomer with a yield of 87%. After removal of the silyl-protecting group, alcohol **14** was oxidized to carboxylic acid **15** in 75% yield using Jones reagent. This reaction was accompanied by formation of ketone **16** in 15% yield via carbon−carbon bond cleavage and thus resembled oxidations of related systems reported previously.[38,39] Final exchange of the N-protecting group gave the desired (*E*)-alkene derivative **2** (89% from **15**). Saturated analogue **3** (77%) was then obtained by palladium-catalyzed hydrogenation of **2** during which some Fmoc cleavage was noted.

Application of the above route to Ala-Gly (*E*)-alkene derivative **4** (Figure 2) has been described previously.[26] The corresponding saturated analogue **5** was obtained by directly reducing the *E*/*Z*-mixture of alkenes **17** obtained in the Wittig reaction (Scheme 2), followed by hydroxyl group deprotection, oxidation, and exchange of the N-protecting group (57% yield from **17**).

Initial attempts to synthesize Gly-Phe (*E*)-alkene derivative **6** via the same protocol (Scheme 3), i.e., by reacting phosphonium

salt **21** with chiral aldehyde **22**, gave a 13:10 mixture of (*E*)- and (*Z*)-isomers according to the ^{1}H NMR spectrum of the crude product. After purification by flash chromatography, the (*E*)-alkene was obtained in a yield of only approximately 10%. Most likely, the poor solubility of phosphonium salt **21** in THF contributed to the low yield as a suspension remained even after the addition of base. Attempts to find improved conditions (Supporting Information) were unsuccessful, and an alternative approach to the Gly-Phe isosteres was therefore employed that instead relied on Evans alkylation of an oxazolidinone enolate to establish the C-terminal stereocenter as described by Kelly and co-workers (Scheme 4).[40]

Initial attempts to alkylate **27** with benzyl bromide gave only trace amounts of product, while the chiral auxiliary was mainly cleaved. It was hypothesized that the lithiated carbamate obtained from **27** could interfere in the reaction, and therefore the Boc-protecting group was exchanged to a benzophenone imine, which has been successfully used in other alkylation reactions.[41−44] Alkylation of **28** then proceeded to give **29** with a 70% yield as a 93:7 diastereomeric mixture. It was not possible to separate the diastereomers using flash chromatography, and therefore the remaining steps were performed on the diastereomeric mixture. Thus, oxazolidinone **29** was treated with basic hydrogen peroxide, followed by acidic hydrolysis of the benzophenone imine and protection of the amino group with an Fmoc group. The crude product was purified by flash chromatography, followed by preparative chiral HPLC, affording **6** from **29** with a yield of 66% and >99% ee. Catalytic hydrogenation of **6** then

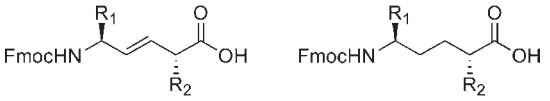

2 R_1 = *i*-Bu, R_2 = Me
4 R_1 = Me, R_2 = H
6 R_1 = H, R_2 = Bn

3 R_1 = *i*-Bu, R_2 = Me
5 R_1 = Me, R_2 = H
7 R_1 = H, R_2 = Bn

Figure 2. Target isostere derivatives protected for use in solid-phase glycopeptide synthesis.

Scheme 2. Saturated Analogue 5 Synthesis[a]

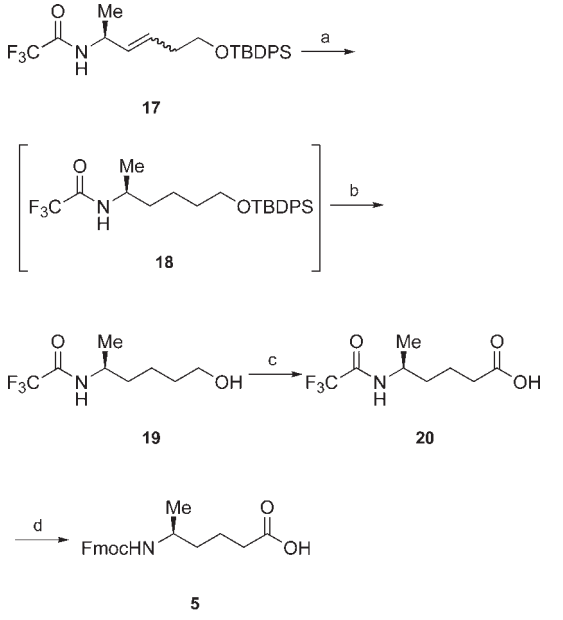

[a] Reagents and conditions: (a) H_2, Pd/C, MeOH, rt; (b) TBAF, THF, rt (71% from **17**); (c) CrO_3, H_2SO_4, acetone/H_2O, rt (88%); (d) (i) K_2CO_3, MeOH/H_2O, rt, (ii) FmocOSu, Na_2CO_3, MeCN/H_2O, rt (92% from **20**).

Scheme 1. Synthesis of Ile-Ala (*E*)-Alkene and Ethylene Derivatives 2 and 3[a]

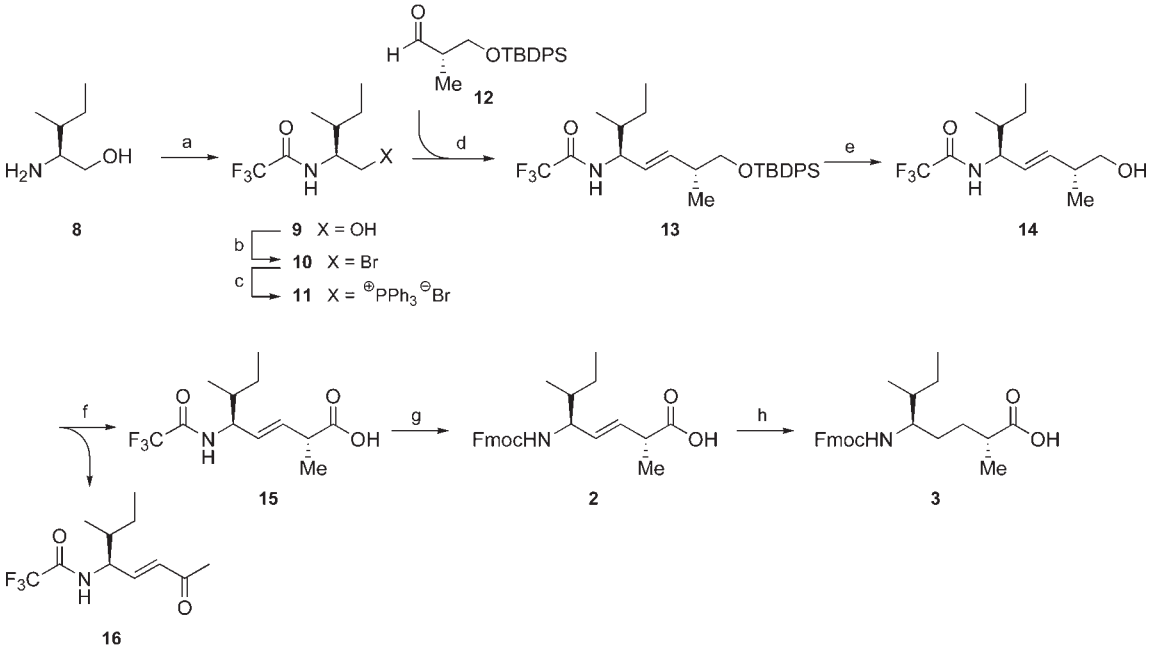

[a] Reagents and conditions: (a) TFAA, Et_3N, CH_2Cl_2, 0 °C (100%); (b) CBr_4, PPh_3, MeCN, 0 °C → rt (85%); (c) PPh_3, toluene, reflux (97%); (d) (i) *n*-BuLi, THF, −78 °C, (ii) aldehyde **12**, THF, −78 °C → 0 °C (87%); (e) TBAF, THF, rt (94%); (f) CrO_3, H_2SO_4, acetone/H_2O, rt (75%); (g) (i) K_2CO_3, MeOH/H_2O, rt, (ii) FmocOSu, Na_2CO_3, MeCN/H_2O, rt (89%); (h) H_2, Pd/C, MeOH, rt (77%).

dx.doi.org/10.1021/ja2038722 |*J. Am. Chem. Soc.* 2011, 133, 14368–14378

also gave the corresponding saturated analogue **7** with a yield of 84%.

The isostere building blocks **2**, **3**, and **5**−**7** were activated using HATU and 2,4,6-collidine and then incorporated into the CII259−273 sequence using Fmoc-based solid-phase glycopeptide synthesis.[46] Cleavage of the isostere glycopeptides from the solid support, deacetylation of the galactose moiety, and final purification by reversed-phase HPLC afforded the trifluoroacetate salts of **31**, **32**, and **34**−**36** (Figure 3) with overall yields of 14−20% based on the resin capacities and in >98% purity. All glycopeptides were homogeneous, according to analytical reversed-phase HPLC using two eluent systems, and their structures were confirmed by ^{1}H NMR spectroscopy and matrix-assisted laser desorption ionization time-of-flight (MALDI-TOF) mass spectrometry. Synthesis of glycopeptide **33** from building block **4** using these conditions has been reported previously.[26]

Binding to the A^q Protein. Competitive binding experiments were performed to investigate the effect of the introduced (*E*)-alkene and ethylene isosteres in **31**−**36** on binding to the A^q protein (Figure 4). It was found that all isostere glycopeptides bound more weakly to A^q than the native **1**. Four of the modified glycopeptides exhibited moderate binding, i.e., the (*E*)-alkenes **31**, **33**, and **35** as well as the Gly-Phe ethylene **36**. The remaining Ile-Ala and Ala-Gly ethylene isosteres **32** and **34** bound weakly. Thus, isosteric replacement of one out of 14 amide bonds in **1** had a profound effect on A^q binding. Selected amide bonds in **1** have previously been replaced by (*E*)-alkene,[26] ketomethylene,[26] methyleneamine,[26] and methylene ether[27] isosteres or oxazole[25] moieties, and these modifications generally resulted in significant effects on binding to A^q and T-cell recognition. Similar observations have also been reported for other murine class II MHC systems.[15,16,18,47−49] In addition, the dramatic effect of disrupting a hydrogen bond between a MHC class II protein and peptides has been studied by selected amino acid mutations of the A^d protein.[50−52]

At two out of the three modified positions (i.e., the Ile-Ala and Ala-Gly positions, Figure 1), stronger A^q binding was obtained for the (*E*)-alkene isostere than the corresponding ethylene isostere (cf., **31** with **32** and **33** with **34**, Figure 4). This agrees with the assumption that an increase in flexibility provided by the ethylenes should lead to a higher entropy cost for binding to A^q and thus result in lower binding affinity.[53,54] Unexpectedly, introduction of the more flexible ethylene isostere at the Gly-Phe position (**36**) resulted in stronger binding to A^q compared to the corresponding (*E*)-alkene (**35**). As both isosteres can mimic the geometry of the native amide, one would expect that the more flexible isostere would bind less strongly than the rigid (*E*)-alkene. However, recent investigations involving thermodynamic analysis, structural and dynamic characterization, and solvation studies of series of ligands binding to proteins[55−58] have shown that the relationship between the enthalpy and entropy components, and their effect on binding affinity, follows a more complex pattern than initially assumed, and as such it is not yet fully understood.

Scheme 3. Attempt to Synthesize Gly-Phe (*E*)-Alkene Derivative 6[a]

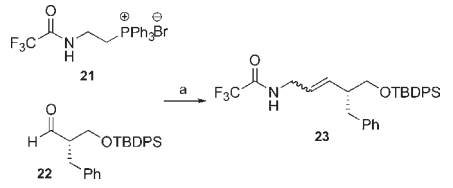

[a] Reagents and conditions: (a) (i) *n*-BuLi, THF or THF/DME 95:5, −78 °C, (ii) aldehyde **22**, THF, −78 °C → 0 °C.

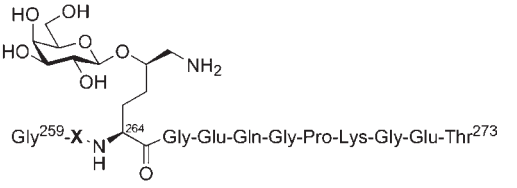

1 X = Ile^{260}-Ala-Gly-Phe^{263}
31 X = **Ile^{260}ψ[(*E*)-CH=CH]Ala^{261}**-Gly-Phe
32 X = **Ile^{260}ψ[CH$_2$CH$_2$]Ala^{261}**-Gly-Phe
33 X = Ile-**Ala^{261}ψ[(*E*)-CH=CH]Gly^{262}**-Phe
34 X = Ile-**Ala^{261}ψ[CH$_2$CH$_2$]Gly^{262}**-Phe
35 X = Ile-Ala-**Gly^{262}ψ[(*E*)-CH=CH]Phe^{263}**
36 X = Ile-Ala-**Gly^{262}ψ[CH$_2$CH$_2$]Phe^{263}**

Figure 3. Native CII259−273 glycopeptide **1** and analogues **31**−**36** modified with (*E*)-alkene and ethylene isosteres.

Scheme 4. Alternative Approach to the Gly-Phe Isosteres[a]

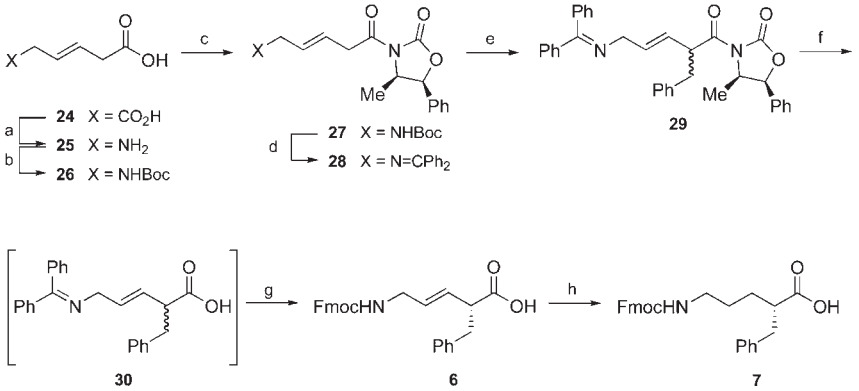

[a] Reagents and conditions: (a) and (b) see Allan et al.;[45] (c) (i) Et$_3$N, *t*BuCOCl, THF, −78 °C, (ii) (4*R*,5*S*)-4-methyl-5-phenyl-2-oxazolidinone, *n*-BuLi, THF, −78 °C → rt (82%); (d) (i) TFA, CH_2Cl_2, rt, (ii) benzophenone imine, CH_2Cl_2, rt (72% from **27**); (e) LDA, BnBr, THF, −78 °C → 0 °C (70% as a mixture with dr 93:7); (f) LiOH, H_2O_2, THF/H_2O, 0 °C; (g) (i) citric acid, THF/H_2O, rt, (ii) FmocOSu, $NaHCO_3$, acetone/H_2O, rt, (iii) chiral chromatography (66% from **28**, 99% ee); (h) H_2, Pd/C, MeOH, rt (84%).

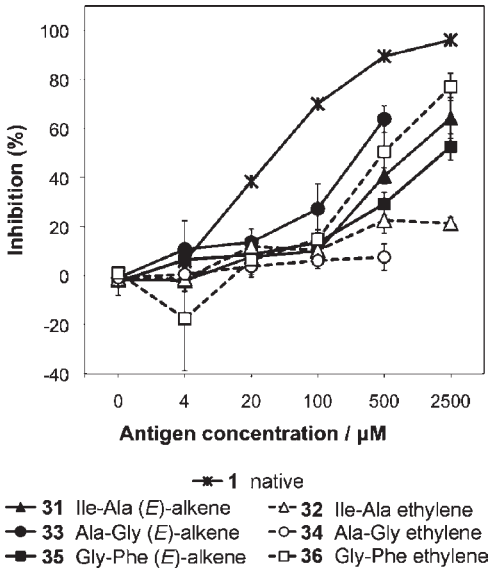

Figure 4. Binding of native **1** and isostere glycopeptides **31**−**36** to A^q. In the competitive binding experiments, increasing concentrations of the glycopeptides **1** or **31**−**36** were incubated with recombinant A^q protein and a fixed concentration of nonglycosylated and biotinylated CII259−273. The amount of biotinylated peptide bound to A^q after incubation was then detected in a time-resolved fluoroimmunoassay using europium-labeled streptavidin. The data are displayed as percent inhibition compared to the biotinylated peptide in the absence of test glycopeptide. The points represent the average of triplicates, and error bars are set to ±1 SD. Percent inhibition values are missing for **33** and **34** at 2.5 mM due to abnormal data.

MD Simulations of Glycopeptide/A^q Complexes. MD simulations were performed to study the dynamics of the glycopeptide/A^q complexes over time. In particular, structural variations and changes in the hydrogen-bonding patterns resulting from the introduced amide bond isosteres were monitored and compared to A^q binding. The stronger A^q binding of the Gly-Phe ethylene isostere **36** compared to the corresponding (*E*)-alkene **35** was specifically addressed.

General Features of the Simulated Complexes. Seven 18 ns MD simulations were performed of complexes between A^q and the native **1** or one of the isostere glycopeptides **31**−**36**. Residues 259−270 of each glycopeptide were included in the simulations, which correspond to the glycopeptide sequence present in the comparative model[25,26] used as the starting structure. The root-mean-square deviation (RMSD) of the backbone C and N atoms from the corresponding initial structures was analyzed over the simulation trajectories to verify the stability of the complexes (Supporting Information). The RMSD profiles were similar for all glycopeptide/A^q complexes and were generally found to plateau within 6 ns, suggesting that a stable equilibrium had been reached.

Visual inspection of frames extracted every 100 ps during the last ns of the simulations showed that all glycopeptides had similar A^q binding modes. As expected, the glycopeptides bound with extended backbone conformations and with the side chains of Ile^{260} and Phe^{263} anchored in the P1 and P4 pockets, respectively. These anchor residues were identified in previous experimental binding studies,[33,59] and the extended peptide backbone is generally observed in crystal structures of class II MHC/peptide complexes.[2] The positions and the conformations of the A^q residues forming the P4 pocket were generally more conserved than those forming the P1 pocket in the extracted frames of the different complexes. This may be because the P4 pocket is defined by both the side chains and backbone of A^q, whereas the P1 pocket is defined by several aromatic side chains. These aromatic side chains seem to be more flexible in their interactions with the glycopeptides.

Table 1. Average and Standard Deviation for the Backbone Dihedral Angle (Defined by $C^{\alpha}-C'-N-C^{\alpha}$) for Each of the Positions Ile^{260}-Ala^{261}, Ala^{261}-Gly^{262}, and Gly^{262}-Phe^{263} for the MD Trajectory between 6 and 18 ns

		dihedral angle (°)	
	glycopeptide (position)	average	±SD
1	(Ile-Ala amide)	179.87	7.24
31	(Ile-Ala (*E*)-alkene)	180.78	5.41
32	(Ile-Ala ethylene)	188.72	13.69
1	(Ala-Gly amide)	172.08	8.35
33	(Ala-Gly (*E*)-alkene)	178.91	5.25
34	(Ala-Gly ethylene)	179.34	13.07
1	(Gly-Phe amide)	170.09	7.40
35	(Gly-Phe (*E*)-alkene)	181.73	5.41
36	(Gly-Phe ethylene)	180.53	11.55

The average values and standard deviations (SD) of the backbone dihedral angles were comparable for the amides, ethylenes, and (*E*)-alkenes at each of the three different positions in the peptides (Table 1 and Supporting Information). Although similar backbone conformations were adopted, the standard deviations of the backbone dihedral angles revealed different degrees of flexibility for the amide and the two isosteres. As would be expected, the (*E*)-alkenes were slightly more rigid when bound to A^q compared to the amides in the native **1**, whereas the ethylenes were more flexible.

Glycopeptide/A^q Hydrogen-Bond Interactions. Analysis of the hydrogen-bonding network for the 259−270 sequence of native **1** between 17 and 18 ns revealed a total of 11 possible interactions with occupancy >5% between the glycopeptide backbone and A^q (Table 2 (for definition of hydrogen bond) and Figure 5). The results resembled the hydrogen-bond pattern displayed in the comparative model[26] of the A^q/CII260−267 complex where 13 possible hydrogen bonds were present; 7 of which were identified in the MD simulations. Although the glycopeptide and the A^q protein were able to form several possible hydrogen bonds during the time of the simulation, not all the bonds were present at a single occasion (snapshot). Six of the hydrogen bonds occurred in more than 40% of the sampled conformations. The average number of hydrogen bonds per snapshot was 5.18 for the 259−270 sequence of **1**, which is far less than the 11 possible. Thus, although the static picture of the peptide/MHC complex based on a comparative model revealed several possible hydrogen bond interactions, the patterns and the strengths of these interactions were found to vary greatly in the dynamic system. The observations that less than half of the possible hydrogen bonds are present as strong hydrogen bonds at any one time and that the patterns varied between the different snapshots are important findings and most likely of critical importance for signaling in the class II MHC/peptide/TCR recognition system.

Most of the possible hydrogen-bond interactions, including 5 of the 6 hydrogen bonds with occupancy higher than 40%, were

Table 2. Hydrogen-Bond Occupancy[a] (in %) between A^q and the 259−270 Glycopeptide Backbones for Native 1 and the Modified Glycopeptides 31−36 for the MD Trajectory between 17 and 18 ns

glycopeptide residue[b]	A^q residue[c]	**1** native	**31** Ile-Ala (*E*)-alkene	**32** Ile-Ala ethylene	**33** Ala-Gly (*E*)-alkene	**34** Ala-Gly ethylene	**35** Gly-Phe (*E*)-alkene	**36** Gly-Phe ethylene
Gly259 (a)	βVal85 (m)	–[d]	–	–	–	14	–	–
Gly259 (a)	βHis81 (s)	53	52	10	–	–	28	6
Gly259 (d)	αSer53 (s)	–	–	12	–	–	–	–
Ile260 (d)	αSer53 (m)	35	–	–	–	–	48	5
Ala261 (d)	βAsn82 (s)	41	modified	modified	53	57	24	35
Ala261 (a)	βAsn82 (s)	72	44	54	modified	modified	69	63
Phe263 (d)	αTyr9 (m)	19	38	7	27	21	modified	modified
Phe263 (a)	αAsn62 (s)	63	–	17	61	58	–	57
Phe263 (a)	αTyr22 (s)	–	57	–	–	–	–	–
Lys264 (d)	βGlu74 (s)	61	–	–	–	–	–	–
Gly265 (d)	αAsn62 (m)	–	–	–	59	30	–	40
Gly265 (d)	αAsn62 (s)	–	–	–	–	–	44	–
Gly265 (a)	αThr65 (s)	–	–	–	–	–	36	13
Glu266 (d)	βTyr30 (s)	8	17	6	55	44	57	46
Glu266 (a)	αAsn69 (s)	17	24	–	–	–	41	–
Gln267 (a)	βTrp61 (s)	74	61	60	70	62	68	70
Gly268 (a)	αHis68 (s)	–	–	–	–	–	25	–
Gly268 (d)	αHis68 (s)	16	22	32	–	–	–	–
Gly268 (d)	αAsn69 (s)	–	–	–	40	35	18	30
Pro269 (a)	αHis68 (s)	–	–	–	–	39	–	–

[a] Calculated with the hydrogen-bond extension in VMD.[60] A hydrogen bond was defined by a donor−acceptor distance of less than 3.3 Å and a donor-H···acceptor angle of less than 20°. Only frequencies >5% are reported. [b] The residue involved in the hydrogen bond is defined as donor (d) or acceptor (a). [c] The hydrogen bond is defined to involve either the side chain (s) or the main chain (m). [d] No hydrogen bond observed or the occupancy is less than 5%.

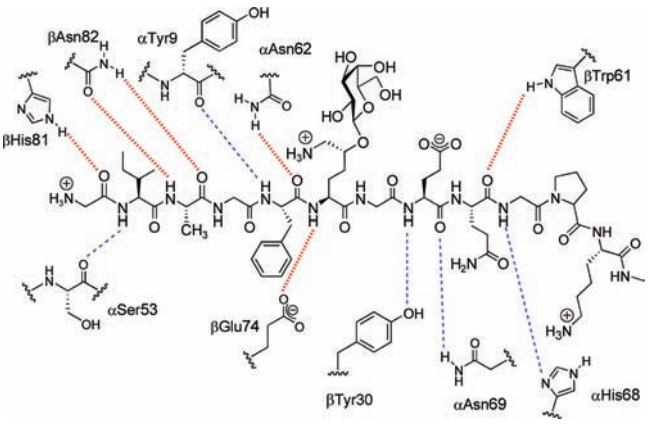

Figure 5. Hydrogen-bond network between the 259−270 backbone sequence of **1** and the A^q protein during the last ns of the MD simulation. The hydrogen-bond interactions (see Table 2 for definition) are illustrated with dashed lines and are color coded according to their occupancy, <40% (blue) and >40% (red).

found in the 259−265 sequence of **1** (Table 2 and Figure 5). Thus, the hydrogen-bonding network between **1** and A^q was mainly formed by the N-terminal part of the glycopeptide and the A^q protein. It should be noted that the 259−265 sequence is almost identical to CII260−267, which was previously identified as the minimal epitope of **1** required for A^q binding and T-cell recognition.[61] The importance of the hydrogen-bonding network in the N-terminal part of a peptide backbone has also been reported for the related mouse class II MHC I-$A^{d\,50-52}$ and human class II MHC HLA-DR systems.[20]

The 3 amide bonds in the Ile^{260}-Phe^{263} sequence of **1**, which were replaced by isosteres in this study, were each involved in one hydrogen-bond interaction with A^q according to the MD data (Table 2 and Figure 5). However, the effect of inserting either (*E*)-alkene or ethylene moieties on A^q binding could not be linked to the occupancy (i.e., the hydrogen-bond strength) of the specific hydrogen bond that was lost. Because the MD simulation of the complex of **1** and A^q revealed a dynamic hydrogen-bonding network, we conducted a more detailed study of the corresponding networks in the complexes of the modified glycopeptides and A^q, focusing on the N-terminal part of the glycopeptides.

Although 7 possible hydrogen bonds were identified between the 259−265 backbone sequence of **1** and residues in A^q, on average only 3.47 interactions were present in each sampled complex conformation (Table 3). A correlation was found between the average number of hydrogen bonds formed between A^q and the "core" 259−265 sequence of the native and modified glycopeptides and the experimentally determined A^q binding. The group of glycopeptides that bound with moderate strength to A^q, i.e., the (*E*)-alkenes **31**, **33**, and **35** as well as the Gly-Phe ethylene **36**, had on average 1.95−2.50 hydrogen bonds between their 259−265 backbone sequences and residues in A^q (Table 3). The Ile-Ala (**32**) and Ala-Gly (**34**) ethylene glycopeptides, which both bound weakly, had 1.25 and 1.84 interactions, respectively. Thus, the loss of hydrogen-bonding interactions in the N-terminal 259−265 sequence of the modified glycopeptides probably contributed to the observed loss of A^q binding. This result is

Table 3. Average Number of Hydrogen Bonds[a] with Standard Deviation Present between A^q and the 259−265 Glycopeptide Backbones for the MD Trajectory between 17 and 18 ns

		number of hydrogen bonds	
	glycopeptide (position)	average	±SD
1	(native)	3.47	1.31
31	(Ile-Ala (*E*)-alkene)	1.95	1.02
32	(Ile-Ala ethylene)	1.25	0.93
33	(Ala-Gly (*E*)-alkene)	2.06	0.98
34	(Ala-Gly ethylene)	1.84	1.02
35	(Gly-Phe (*E*)-alkene)	2.50	1.19
36	(Gly-Phe ethylene)	2.19	1.02

[a] Calculated with the hydrogen-bond extension in VMD.[60] A hydrogen bond was defined by a donor−acceptor distance of less than 3.3 Å and a donor-H···acceptor angle of less than 20°.

Table 4. Average RMSD[a] for the α1 and β1 Helices of A^q in Complex with Glycopeptides 1 and 31−36, Respectively, for the MD Trajectory between 9 and 18 ns

		RMSD α1 helix		RMSD β1 helix	
	glycopeptide	average	±SD	average	±SD
1	(native)	1.59	0.42	1.10	0.14
31	(Ile-Ala (*E*)-alkene)	3.26	0.31	1.66	0.18
32	(Ile-Ala ethylene)	2.50	0.25	1.40	0.19
33	(Ala-Gly (*E*)-alkene)	3.24	0.25	1.26	0.22
34	(Ala-Gly ethylene)	2.98	0.20	1.42	0.16
35	(Gly-Phe (*E*)-alkene)	2.82	0.28	1.49	0.24
36	(Gly-Phe ethylene)	2.80	0.25	1.21	0.14

[a] RMSD calculated with frame 1 as reference in the respective simulation.

supported by earlier studies which showed that for peptides binding to MHC class I molecules, the distribution of medium and strong hydrogen bonds determined by short (200 ps) MD simulations correlated with the binding potency of the peptides.[62]

The analysis of the 259−265 fragments revealed that the amide bond isosteres did not solely affect the hydrogen-bonding interactions at the positions where they were introduced. In fact, the different isosteres substantially altered the hydrogen-bonding network along their glycopeptide backbones compared to the native **1** (Table 2). These altered networks also affected the dynamics and the structure of the helices that enclose the binding site. The α1 helix of A^q in the complexes with the isosteres adopted different conformations compared to the complex with **1** (cf. average RMSD values in Table 4). The β1 helix of A^q in the complexes with the isosteres also adopted different conformations compared to the native complex, although the effect was not as profound as for the α1 helix. In addition, the α1 helix of A^q in the complex with **1** was more flexible than the β1 helix over the simulation time (cf. SD for RMSD values in Table 4). Interestingly, the helices of A^q in complex with isosteres showed a different dynamic pattern, where the α1 helices were more rigid and the β1 helices were slightly more flexible compared to the native complex.

In summary, we found that the hydrogen-bonding network between A^q and bound glycopeptides is highly dynamic over time. Only half of the possible number of hydrogen bonds between A^q and **1** were present in single snapshots, the majority of which were found in the N-terminal 259−265 sequence of **1**. We also observed that site-specific introduction of an isostere that necessitates the loss of one hydrogen-bond interaction had a profound effect on the complete hydrogen-bonding network between the N-terminal part of the glycopeptide backbone and the A^q protein. The results from the MD study presented herein show that these hydrogen bonds are strongly coupled to each other. This finding is consistent with previous reports that suggest the hydrogen-bond network formed between peptides and class II MHC proteins follows a cooperative model in which the strength and the presence of individual bonds are dependent upon the integrity of neighboring interactions.[2,50−52]

Structural Changes in the Gly-Phe Ethylene Complex. The A^q binding data revealed that the glycopeptide with an ethylene isostere at the Gly-Phe position unexpectedly bound more strongly to A^q than the corresponding (*E*)-alkene (cf. **36** and **35** in Figure 4), which is in contrast to the trend observed when the isosteres were inserted at the two other positions. This difference in binding is probably due to an improved A^q binding of the ethylene isostere in the Gly-Phe position compared to the other two positions rather than decreased binding strength of the corresponding (*E*)-alkene. This is because similar interaction patterns with A^q were observed for **35** as for alkenes **31** and **33**, and no conformational strain of the proposed bioactive conformation of **35** could be detected. The improved binding of **36** compared to **35** could be driven by enthalpy and/or entropy. In the analysis of the trajectories no profound difference in movements (flexibility) could be detected between the three ethylenes or between the three alkenes when bound to A^q. Furthermore, in this particular case it seems that the relative enthalpic and entropic effects of water were small because the solvent accessible surface of the complexes of the six isosteres and the native **1** at the three modified positions were similar throughout the MD simulation. Based on these observations, together with the assumption that the isostere glycopeptides have similar flexibility and solvation in their unbound states, we suggest that the relative difference in entropy between the different isosteres is too small to account for the stronger binding of the Gly-Phe ethylene **36**, compared to the corresponding (*E*)-alkene **35**. Instead, the stronger binding of the Gly-Phe ethylene **36** could be mainly enthalpy driven and directly dependent on molecular interactions between **36** and A^q.

A main difference between the hydrogen-bonding network involving the 259−265 sequences of Gly-Phe ethylene **36** and (*E*)-alkene **35** was that the hydrogen bond between Phe^{263} and αAsn62 of A^q was preserved in **36** to the same extent as observed for **1**, whereas this interaction was not observed in the complex with the more rigid (*E*)-alkene **35**. At the same time, the side chain of αAsn62 formed a hydrogen bond to Gly^{265} in **35**, which was not observed for **36**, whereas the main chain of αAsn62 interacted with Gly^{265} in **36**, which was not observed for **35**. Furthermore, two hydrogen bonds (between Gly^{259} and βHis81 and Ile^{260} and αSer53, Table 2) at the N-terminal were weakened for **36** compared to **35**. Further analysis of the MD trajectories revealed that the A^q/**36** complex adopted an equilibrium conformation that was structurally different to the equilibrium conformations of the other A^q/glycopeptide complexes (Table 5 and Supporting Information). This structural difference could be

Table 5. Average RMSD for the Sequence Ile^{260}-Phe^{263} and χ^1 Dihedral Angle for Phe^{263} Calculated for the MD Trajectory between 6 and 18 ns

		RMSD heavy atoms of Ile^{260}-Phe^{263} (Å)[a]		dihedral angle χ^1 (°) of the Phe side chain	
	glycopeptide	average	±SD	average	±SD
1	(native)	1.18	0.21	−80.48	9.22
31	(Ile-Ala (*E*)-alkene)	1.33	0.27	−77.08	12.17
32	(Ile-Ala ethylene)	1.31	0.19	−75.16	9.55
33	(Ala-Gly (*E*)-alkene)	1.08	0.16	−73.20	7.72
34	(Ala-Gly ethylene)	1.08	0.17	−76.83	8.49
35	(Gly-Phe (*E*)-alkene)	0.91	0.15	−78.59	9.38
36	(Gly-Phe ethylene)	2.11	0.27	−101.79	13.43

[a] RMSD calculated with frame 1 as reference in the respective simulation.

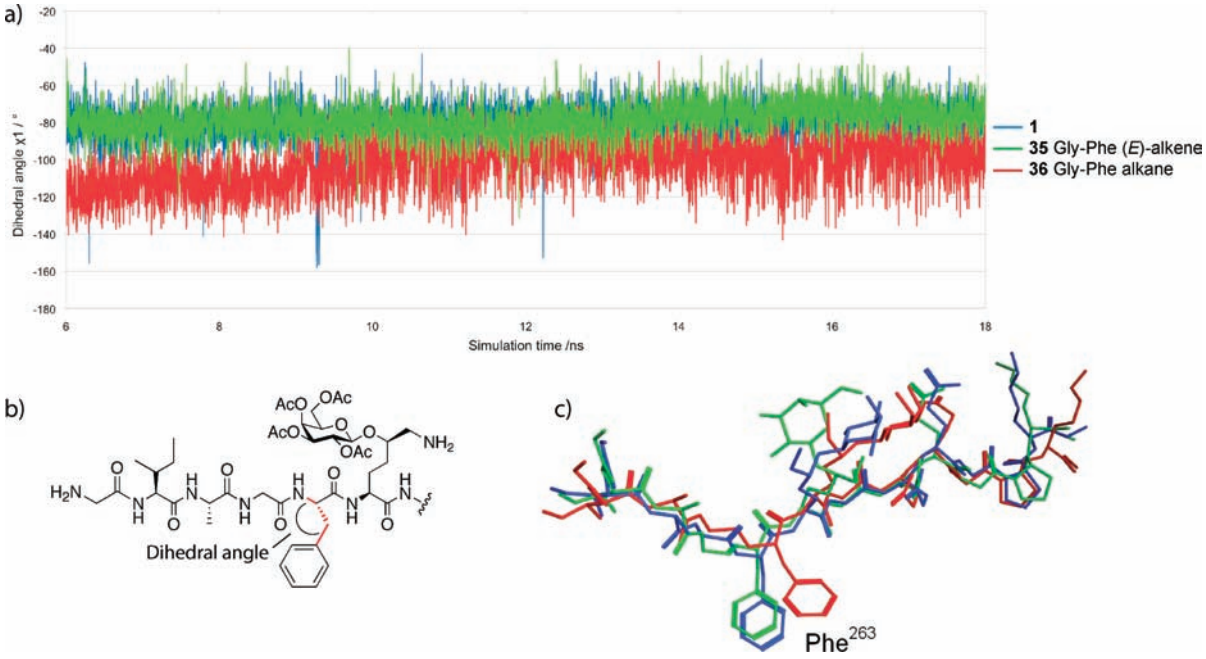

Figure 6. (a) Dihedral angle χ^1 in the Phe^{263} residue versus simulation time (from 6 to 18 ns) for native **1**, Gly-Phe (*E*)-alkene **35**, and Gly-Phe ethylene **36**. (b) Observed χ^1 dihedral angle in the Phe^{263} residue illustrated for **1**, defined by the bonds between the atoms N−Cα−Cβ−Cδ. Individual curves of the dihedral angles for all glycopeptides are presented in the Supporting Information. (c) Example of superposed binding poses of glycopeptides **1** (blue), **35** (green), and **36** (red). The poses were selected at the end of the 18 ns simulation trajectory from complexes with an average RMSD for the backbone heavy atoms.

traced to the Phe^{263} side chain in **36**, whose dihedral angle χ^1 differed significantly from the corresponding angles in the native **1** and the other isosteres **31**−**35** (Table 5, Figure 6, and Supporting Information). As mentioned earlier, the side chain of the Phe^{263} residue is an important anchor that interacts with the P4 pocket of A^q. Snapshots extracted from the simulation trajectories from 17 to 18 ns showed that the altered dihedral angle χ^1 in **36** corresponded to a shift of the Phe side chain in the P4 pocket (Figure 6). This allowed the Phe side chain to make new interactions with residues in the P4 pocket, e.g., βTyr30, βPhe40, and βPhe47, while at the same time some interactions were weakened, e.g., with βVal78. It is possible that the flexibility provided by the ethylene, which enabled the repositioning of the Phe side chain in the P4 pocket, also allowed the Phe^{263}-αAsn62 hydrogen bond to be preserved in the A^q complex with **36**. One may speculate that the increased binding strength of the complex may be due to a cooperative effect of the van der Waals interactions formed by the anchor residues of the glycopeptide and the protein and the hydrogen-bonding network. Such cooperative binding has recently been described for a series of thrombin inhibitors.[63] In summary, the altered interactions between Phe^{263} of **36** and the A^q residues forming the P4 pocket, together with the hydrogen-bonding network, may result in a more favorable free energy of binding for **36** to A^q compared to **35**.

T-Cell Recognition. The ability of the isostere-modified glycopeptides to stimulate four A^q-restricted T-cell hybridomas,[64] selected from groups with different specificities for the galactose moiety of **1**,[32] was investigated in an assay of IL-2 secretion (Figure 7). In general, T-cell stimulation is determined by the strength of peptide binding to the class II MHC as well as by the epitope displayed by the peptide/MHC complex to the TCR. In this study, the native **1** induced similar strong response profiles

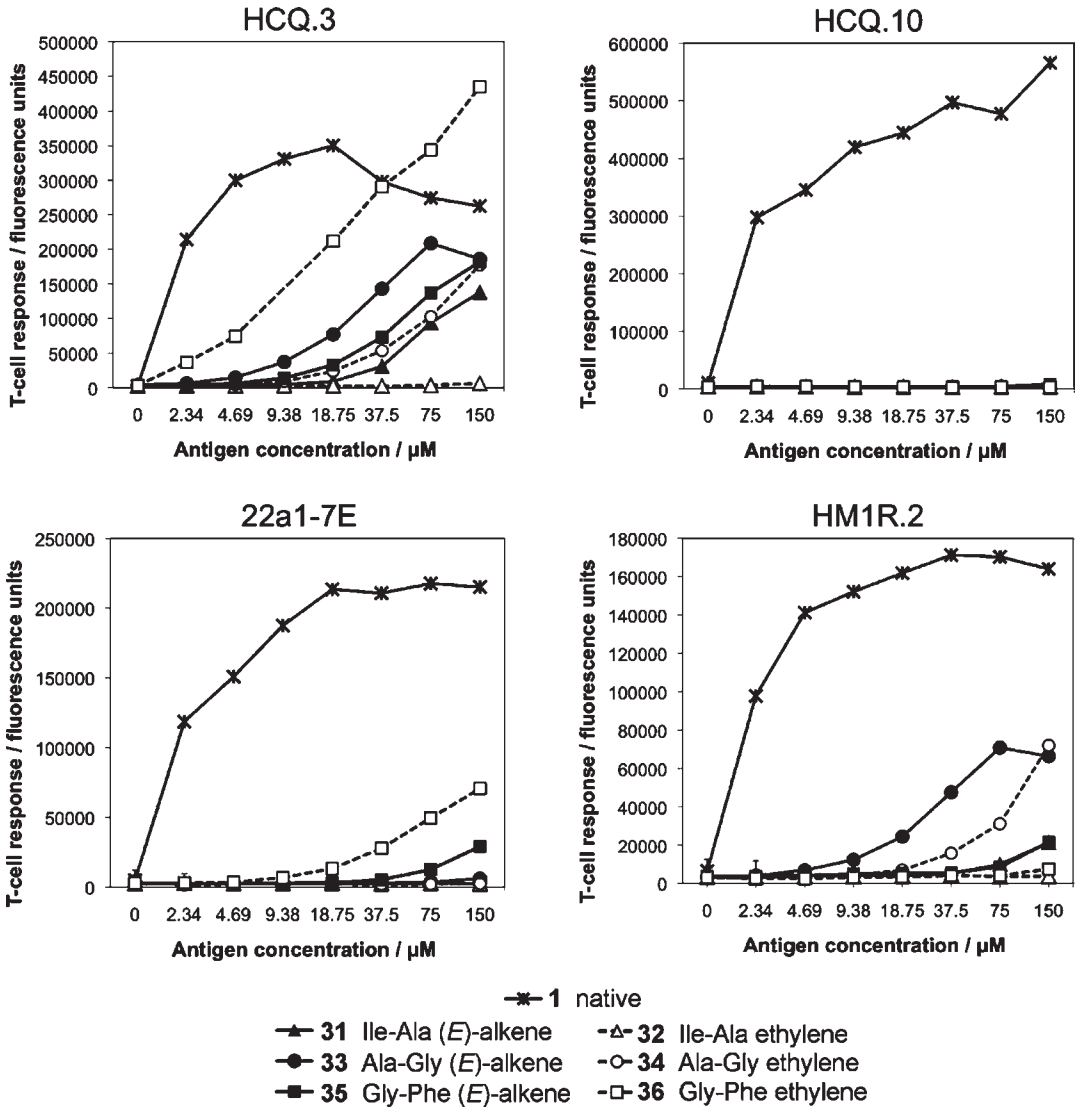

Figure 7. Response of the A^q-restricted T-cell hybridomas HCQ.3, HCQ.10, 22a1-7E, and HM1R.2 to glycopeptides **1** and **31**−**36**. The hybridomas were evaluated by incubation with syngeneic spleen cells and increasing concentrations of **1** or **31**−**36**. T-cell hybridomas that recognize glycopeptides bound to A^q on the spleen cells secreted IL-2, which was quantified by a sandwich ELISA using the DELFIA system. The points represent the average of duplicates. The fluorescence value for **36** at 9.38 μM for the HCQ.3 hybridoma is not reported due to a technical error when performing the assay.

for all four T-cell hybridomas. The (*E*)-alkene- and ethylene-modified glycopeptides elicited weaker responses than **1** which, at least partly, should be a result of their weaker binding to A^q. The altered epitope that results from changes in the structure and the dynamics of the α1 and β1 helices in A^q in the complexes with the modified glycopeptides most likely provides another explanation for the reduced responses. In addition, the four hybridomas displayed very different response profiles for the modified glycopeptides, indicating that their TCRs have different specificities for the presented A^q/glycopeptide epitopes. Hybridoma HCQ.3 recognized all modified glycopeptides except Ile-Ala ethylene **32,** and generally the responses reflected how well the glycopeptides bound to A^q. In contrast, HCQ.10 did not recognize any of the modified glycopeptides. Hybridoma 22a1-7E recognized only the two Gly-Phe modified glycopeptides **35** and **36** weakly, whereas HM1R.2 mainly recognized the two Ala-Gly modified glycopeptides **33** and **34**, indicating that differences in the presented epitopes determine which glycopeptides are recognized by these two hybridomas.

The Ile-Ala ethylene **32** was the only glycopeptide that was not recognized by any of the T-cell hybridomas. The MD simulations showed that the Ile side chain of this glycopeptide was not positioned as deeply in the P1 pocket as in the complexes with the other glycopeptides. This could be due to the high flexibility of the ethylene isostere and the loss of hydrogen-bond interactions, which probably alters the presentation of the epitope to such an extent that T-cell recognition is completely abolished. Changes in peptide structure that alter the epitope displayed to the TCR, and in so doing dramatically influence T-cell recognition, have been described previously for a peptide bound by the related murine $I\text{-}E^k$ protein.[65] Furthermore, we have previously correlated differences in the presented epitope and the dynamics of the glycopeptide/A^q complex to different T-cell responses for glycopeptides with the Ile^{260} and Phe^{263} residues substituted with non-natural amino acids.[11] Previous reports have indicated that the kinetics of the TCR's interaction with the class II MHC/peptide complex is a major determinant for T-cell activity.[66−70] It

dx.doi.org/10.1021/ja2038722 |*J. Am. Chem. Soc.* 2011, 133, 14368–14378

is also likely that the dissociation rate of the TCR's interaction with the (*E*)-alkene- and ethylene-modified glycopeptides is an important factor determining the T-cell responses observed in this study. Furthermore, the different and dynamic hydrogen-bond networks revealed by the MD studies may affect the presentation of the glycopeptides by A^q and consequently TCR recognition.

CONCLUSIONS

In this study the amides at positions Ile^{260}-Ala^{261}, Ala^{261}-Gly^{262}, and Gly^{262}-Phe^{263} in the CII259−273 (**1**) glycopeptide backbone were replaced by (*E*)-alkene and ethylene amide bond isosteres to probe the effect of altering the hydrogen-bonding capability on binding to the A^q class II MHC protein. Competitive binding experiments revealed that modifying one out of 14 amide bonds in glycopeptide **1** reduced binding to A^q to a greater extent than expected. Differences in the stability of the glycopeptide/A^q complexes were investigated by MD simulations, which showed a dynamic network of hydrogen bonds between the glycopeptide backbone and A^q.

The A^q/**1** complex displayed a lower number of hydrogen bonds in each snapshot than both the total number of possible hydrogen bonds observed during the simulation and the number reported for a static model of the complex published recently.[26] Thus, the introduced amide bond isosteres affected a smaller hydrogen-bonding network than initially anticipated, providing one possible explanation for the unexpectedly large reduction in A^q binding. In addition, the MD simulations revealed that it was primarily the N-terminal CII259−265 backbone sequence that was involved in an extensive network of strong hydrogen-bond interactions with A^q. This network was substantially altered by the position and the nature of the introduced amide bond isosteres, suggesting that a cooperative effect was responsible for the reduction in binding. These findings are in close agreement with previous reports of dense and cooperative hydrogen-bonding networks in N-terminal parts of peptides bound by the mouse class II MHC $A^{d\ 50-52}$ and human class II MHC HLA-DR proteins.[20]

As expected, glycopeptides with the more rigid (*E*)-alkene isostere were more strongly bound to A^q than glycopeptides with the ethylene isosteres at the Ile-Ala and Ala-Gly positions. Interestingly, the opposite relationship was found for the Gly-Phe position, where the ethylene isostere bound more strongly to A^q than the corresponding (*E*)-alkene. MD simulations revealed that the increased flexibility of the ethylene isostere enabled repositioning of the Phe side chain in the P4 pocket and allowed the Phe^{263}-αAsn62 hydrogen bond to be maintained, in contrast to the corresponding (*E*)-alkene.

Finally, the isostere-modified glycopeptides significantly affected the interactions with four different T-cell hybridomas, specific for CII259−273. A general reduction in T-cell response was observed for all modified glycopeptides, which was assumed to be due to the reduction in A^q binding and to structural and dynamic changes in the α1 and β1 helices of A^q. The very different response profiles that were displayed by the hybridomas were most likely caused by differences in the hydrogen-bonding networks and the secondary effects thereof, resulting in the presentation of different glycopeptide/A^q epitopes to the TCRs. The dynamic variation of the patterns and the strengths of the hydrogen-bond interactions in the class II MHC/glycopeptide complexes plays a crucial role in determining if an immune response is initiated via activation of the T-cell.

ASSOCIATED CONTENT

Supporting Information. Full experimental details for synthesis of all compounds, the MHC-binding assay and the T-cell recognition assay, details for the MD simulations, NMR spectra for all new isolated compounds, A^q binding curves for triplicates, complete ref 20, RMSD for A^q/glycopeptide complexes vs simulation time, backbone dihedral angle for **1**, **31**, **33**, and **35** vs simulation time, backbone dihedral angle for **1**, **32**, **34**, and **36** vs simulation time, RMSD for Ile^{260}-Phe^{263} sequences vs simulation time, Phe dihedral angles vs simulation time, and RMSD of the α1 and β1 helices of A^q vs simulation time. This material is available free of charge via the Internet at http://pubs.acs.org.

AUTHOR INFORMATION

Corresponding Author
anna.linusson@chem.umu.se; jan.kihlberg@chem.umu.se

ACKNOWLEDGMENT

This work was funded by grants from the Swedish Research Council (dnr 2008-3672), the Swedish Strategic Science Foundation (SSF), the JC Kempe Foundation (SJCKMS), and the EU project Masterswitch HEALTH-F2-2008-223404. The MD simulations were conducted using the resources of the High Performance Computing Center North (HPC2N).[71] The authors thank Anna Johansson at AstraZeneca R&D Mölndal for chiral HPLC purification of compound **6**.

REFERENCES

(1) Janeway, C. A.; Travers, P.; Walport, M.; Shlomchik, M. J. *Immunobiology*; 6th ed.; Garland Science Publishing: Oxford, U.K., 2005.
(2) McFarland, B. J.; Beeson, C. *Med. Res. Rev.* **2002**, *22*, 168–203.
(3) Stern, L. J.; Brown, J. H.; Jardetzky, T. S.; Gorga, J. C.; Urban, R. G.; Strominger, J. L.; Wiley, D. C. *Nature* **1994**, *368*, 215–221.
(4) Yaneva, R.; Springer, S.; Zacharias, M. *Biopolymers* **2009**, *91*, 14–27.
(5) Weber, P.; Raynaud, I.; Ettouati, L.; Trescol-Biemont, M. C.; Carrupt, P. A.; Paris, J.; Rabourdin-Combe, C.; Gerlier, D.; Testa, B. *Int. Immunol.* **1998**, *10*, 1753–1764.
(6) Knapp, B.; Omasits, U.; Bohle, B.; Maillere, B.; Ebner, C.; Schreiner, W.; Jahn-Schmid, B. *Mol. Immunol.* **2009**, *46*, 1839–1844.
(7) Knapp, B.; Omasits, U.; Schreiner, W.; Epstein, M. M. *PLoS One* **2010**, *5*, e11653.
(8) Toh, H.; Kamikawaji, N.; Tana, T.; Muta, S.; Sasazuki, T.; Kuhara, S. *Protein Eng.* **2000**, *13*, 423–429.
(9) Toh, H.; Kamikawaji, N.; Tana, T.; Sasazuki, T.; Kuhara, S. *Protein Eng.* **1998**, *11*, 1027–1032.
(10) Wan, S.; Flower, D. R.; Coveney, P. V. *Mol. Immunol.* **2008**, *45*, 1221–1230.
(11) Andersson, I. E.; Andersson, C. D.; Batsalova, T.; Dzhambazov, B.; Holmdahl, R.; Kihlberg, J.; Linusson, L. *PLoS One* **2011**, *6*, e17881.
(12) De Rosa, M. C.; Giardina, B.; Bianchi, C.; Alinovi, C. C.; Pirolli, D.; Ferraccioli, G.; De Santis, M.; Di Sante, G.; Ria, F. *PLoS One* **2010**, *5*, e11550.
(13) Smilek, D. E.; Wraith, D. C.; Hodgkinson, S.; Dwivedy, S.; Steinman, L.; McDevitt, H. O. *Proc. Natl. Acad. Sci. U.S.A.* **1991**, *88*, 9633–9637.

(14) Gautam, A. M.; Lock, C. B.; Smilek, D. E.; Pearson, C. I.; Steinman, L.; McDevitt, H. O. *Proc. Natl. Acad. Sci. U.S.A.* **1994**, *91*, 767–771.
(15) Ettouati, L.; Salvi, J. P.; Trescol-Biémont, M. C.; Walchshofer, N.; Gerlier, D.; Rabourdin-Combe, C.; Paris, J. *Pept. Res.* **1996**, *9*, 248–253.
(16) Mézière, C.; Viguier, M.; Dumortier, H.; Lo-Man, R.; Leclerc, C.; Guillet, J. G.; Briand, J. P.; Muller, S. *J. Immunol.* **1997**, *159*, 3230–3237.
(17) Cotton, J.; Hervé, M.; Pouvelle, S.; Maillère, B.; Ménez, A. *Int. Immunol.* **1998**, *10*, 159–166.
(18) Ettouati, L.; Casimir, J. R.; Raynaud, I.; Trescol-Biémont, M. C.; Carrupt, P. A.; Gerlier, D.; Rabourdin-Combe, C.; Testa, B.; Paris, J. *Protein Pept. Lett.* **1998**, *5*, 221–229.
(19) Smith, A. B., III; Benowitz, A. B.; Sprengeler, P. A.; Barbosa, J.; Guzman, M. C.; Hirschmann, R.; Schweiger, E. J.; Bolin, D. R.; Nagy, Z.; Campbell, R. M.; Cox, D. C.; Olson, G. L. *J. Am. Chem. Soc.* **1999**, *121*, 9286–9298.
(20) Bolin, D. R.; et al. *J. Med. Chem.* **2000**, *43*, 2135–2148.
(21) Hart, M.; Beeson, C. *J. Med. Chem.* **2001**, *44*, 3700–3709.
(22) Koehler, N. K. U.; Yang, C. Y.; Varady, J.; Lu, Y.; Wu, X.; Liu, M.; Yin, D.; Bartels, M.; Xu, B.; Roller, P. P.; Long, Y.; Li, P.; Kattah, M.; Cohn, M. L.; Moran, K.; Tilley, E.; Richert, J. R.; Wang, S. *J. Med. Chem.* **2004**, *47*, 4989–4997.
(23) Rosloniec, E. F.; Brandstetter, T.; Leyer, S.; Schwaiger, F. W.; Nagy, Z. A. *J. Autoimmunity* **2006**, *27*, 182–195.
(24) Boots, A. M. H.; Hubers, H.; Kouwijzer, M.; Zandbrink, L. D.; Westrek-Esselink, B. M.; van Doorn, C.; Stenger, R.; Bos, E. S.; van Lierop, M. J. C.; Verheijden, G. F.; Timmers, C. M.; van Staveren, C. J. *Arthritis Res. Ther.* **2007**, *9*, R71.
(25) Andersson, I. E.; Batsalova, T.; Dzhambazov, B.; Edvinsson, L.; Holmdahl, R.; Kihlberg, J.; Linusson, A. *Org. Biomol. Chem.* **2010**, *8*, 2931–2940.
(26) Andersson, I. E.; Dzhambazov, B.; Holmdahl, R.; Linusson, A.; Kihlberg, J. *J. Med. Chem.* **2007**, *50*, 5627–5643.
(27) Holm, L.; Bockermann, R.; Wellner, E.; Bäcklund, J.; Holmdahl, R.; Kihlberg, J. *Bioorg. Med. Chem.* **2006**, *14*, 5921–5932.
(28) Bäcklund, J.; Treschow, A.; Bockermann, R.; Holm, B.; Holm, L.; Issazadeh-Navikas, S.; Kihlberg, J.; Holmdahl, R. *Eur. J. Immunol.* **2002**, *32*, 3776–3784.
(29) Dzhambazov, B.; Nandakumar, K. S.; Kihlberg, J.; Fugger, L.; Holmdahl, R.; Vestberg, M. *J. Immunol.* **2006**, *176*, 1525–1533.
(30) Bäcklund, J.; Carlsen, S.; Höger, T.; Holm, B.; Fugger, L.; Kihlberg, J.; Burkhardt, H.; Holmdahl, R. *Proc. Natl. Acad. Sci. U.S.A.* **2002**, *99*, 9960–9965.
(31) Broddefalk, J.; Forsgren, M.; Sethson, I.; Kihlberg, J. *J. Org. Chem.* **1999**, *64*, 8948–8953.
(32) Holm, B.; Bäcklund, J.; Recio, M. A. F.; Holmdahl, R.; Kihlberg, J. *ChemBioChem* **2002**, *3*, 1209–1222.
(33) Kjellén, P.; Brunsberg, U.; Broddefalk, J.; Hansen, B.; Vestberg, M.; Ivarsson, I.; Engström, Å.; Svejgaard, A.; Kihlberg, J.; Fugger, L.; Holmdahl, R. *Eur. J. Immunol.* **1998**, *28*, 755–767.
(34) Venkatesan, N.; Kim, B. H. *Curr. Med. Chem.* **2002**, *9*, 2243–2270.
(35) Wiktelius, D.; Luthman, K. *Org. Biomol. Chem.* **2007**, *5*, 603–605.
(36) Ley, S. V.; Anthony, N. J.; Armstrong, A.; Brasca, M. G.; Clarke, T.; Culshaw, D.; Greck, C.; Grice, P.; Jones, A. B.; Lygo, B.; Madin, A.; Sheppard, R. N.; Slawin, A. M. Z.; Williams, D. J. *Tetrahedron* **1989**, *45*, 7161–7194.
(37) Guan, Y. C.; Wu, J. L.; Sun, L.; Dai, W. M. *J. Org. Chem.* **2007**, *72*, 4953–4960.
(38) He, J. F.; Wu, Y. L. *Tetrahedron* **1988**, *44*, 1933–1940.
(39) Platzek, J.; Snatzke, G. *Tetrahedron* **1987**, *43*, 4947–4968.
(40) Fu, Y.; Bieschke, J.; Kelly, J. W. *J. Am. Chem. Soc.* **2005**, *127*, 15366–15367.
(41) Odonnell, M. J.; Bennett, W. D.; Bruder, W. A.; Jacobsen, W. N.; Knuth, K.; Leclef, B.; Polt, R. L.; Bordwell, F. G.; Mrozack, S. R.; Cripe, T. A. *J. Am. Chem. Soc.* **1988**, *110*, 8520–8525.
(42) Ooi, T.; Kameda, M.; Taniguchi, M.; Maruoka, K. *J. Am. Chem. Soc.* **2004**, *126*, 9685–9694.
(43) Maruoka, K.; Tayama, E.; Ooi, T. *Proc. Natl. Acad. Sci. U.S.A.* **2004**, *101*, 5824–5829.
(44) Chandra, A.; Viswanathan, R.; Johnston, J. N. *Org. Lett.* **2007**, *9*, 5027–5029.
(45) Allan, R. D.; Dickenson, H. W.; Johnston, G. A. R.; Kazlauskas, R.; Tran, H. W. *Aust. J. Chem.* **1985**, *38*, 1651–1656.
(46) Atherton, E.; Sheppard, R. C. *Solid phase peptide synthesis*. IRL Press at Oxford University Press: Oxford, U.K., 1989.
(47) Herve, M.; Maillere, B.; Mourier, G.; Texier, C.; Leroy, S.; Menez, A. *Mol. Immunol.* **1997**, *34*, 157–163.
(48) Cotton, J.; Herve, M.; Pouvelle, S.; Maillere, B.; Menez, A. *Int. Immunol.* **1998**, *10*, 159–166.
(49) de Haan, E. C.; Wauben, M. H. M.; Grosfeld-Stulemeyer, M. C.; Kruijtzer, J. A. W.; Liskamp, R. M. J.; Moret, E. E. *Bioorg. Med. Chem.* **2002**, *10*, 1939–1945.
(50) McFarland, B. J.; Katz, J. F.; Beeson, C.; Sant, A. J. *Proc. Natl. Acad. Sci. U.S.A.* **2001**, *98*, 9231–9236.
(51) McFarland, B. J.; Katz, J. F.; Sant, A. J.; Beeson, C. *J. Mol. Biol.* **2005**, *350*, 170–183.
(52) McFarland, B. J.; Beeson, C.; Sant, A. J. *J. Immunol.* **1999**, *163*, 3567–3571.
(53) Cram, D. J. *Angew. Chem., Int. Ed.* **1986**, *25*, 1039–1134.
(54) Houk, K. N.; Leach, A. G.; Kim, S. P.; Zhang, X. Y. *Angew. Chem., Int. Ed.* **2003**, *42*, 4872–4897.
(55) Diehl, C.; Engström, O.; Delaine, T.; Håkansson, M.; Genheden, S.; Modig, K.; Leffler, H.; Ryde, U.; Nilsson, U. J.; Akke, M. *J. Am. Chem. Soc.* **2010**, *132*, 14577–14589.
(56) DeLorbe, J. E.; Clements, J. H.; Teresk, M. G.; Benfield, A. P.; Plake, H. R.; Millspaugh, L. E.; Martin, S. F. *J. Am. Chem. Soc.* **2009**, *131*, 16758–16770.
(57) Baum, B.; Muley, L.; Smolinski, M.; Heine, A.; Hangauer, D.; Klebe, G. *J. Mol. Biol.* **2010**, *397*, 1042–1054.
(58) Ward, J. M.; Gorenstein, N. M.; Tian, J. H.; Martin, S. F.; Post, C. B. *J. Am. Chem. Soc.* **2010**, *132*, 11058–11070.
(59) Rosloniec, E. F.; Whittington, K. B.; Brand, D. D.; Myers, L. K.; Stuart, J. M. *Cell. Immunol.* **1996**, *172*, 21–28.
(60) Humphrey, W.; Dalke, A.; Schulten, K. *J. Mol. Graphics* **1996**, *14*, 33–38.
(61) Holm, L.; Kjellén, P.; Holmdahl, R.; Kihlberg, J. *Bioorg. Med. Chem.* **2005**, *13*, 473–482.
(62) Rognan, D.; Krebs, S.; Kuonen, O.; Lamas, J. R.; deCastro, J. A. L.; Folkers, G. *J. Comput.-Aided Mol. Des.* **1997**, *11*, 463–478.
(63) Muley, L.; Baum, B.; Smolinski, M.; Freindorf, M.; Heine, A.; Klebe, G.; Hangauer, D. G. *J. Med. Chem.* **2010**, *53*, 2126–2135.
(64) Corthay, A.; Bäcklund, J.; Broddefalk, J.; Michaëlsson, E.; Goldschmidt, T. J.; Kihlberg, J.; Holmdahl, R. *Eur. J. Immunol.* **1998**, *28*, 2580–2590.
(65) Kersh, G. J.; Miley, M. J.; Nelson, C. A.; Grakoui, A.; Horvath, S.; Donermeyer, D. L.; Kappler, J.; Allen, P. M.; Fremont, D. H. *J. Immunol.* **2001**, *166*, 3345–3354.
(66) Kersh, G. J.; Kersh, E. N.; Fremont, D. H.; Allen, P. M. *Immunity* **1998**, *9*, 817–826.
(67) Lyons, D. S.; Lieberman, S. A.; Hampl, J.; Boniface, J. J.; Chien, Y. H.; Berg, L. J.; Davis, M. M. *Immunity* **1996**, *5*, 53–61.
(68) Matsui, K.; Boniface, J. J.; Steffner, P.; Reay, P. A.; Davis, M. M. *Proc. Natl. Acad. Sci. U.S.A.* **1994**, *91*, 12862–12866.
(69) McKeithan, T. W. *Proc. Natl. Acad. Sci. U.S.A.* **1995**, *92*, 5042–5046.
(70) Rabinowitz, J. D.; Beeson, C.; Lyons, D. S.; Davis, M. M.; McConnell, H. M. *Proc. Natl. Acad. Sci. U.S.A.* **1996**, *93*, 1401–1405.
(71) *High Performance Computing Center North (HPC2N)*; HPC2N: Umeå, Sweden; www.hpc2n.umu.se/ (accessed Apr 27, 2011).